Shifts and widths of Feshbach resonances in atomic waveguides

Shahpoor Saeidian,[1,*] Vladimir S. Melezhik,[2,†] and Peter Schmelcher[3,‡]

[1]*Optics and Photonics Research Center, Department of Physics, Institute for Advanced Studies in Basic Sciences (IASBS), Gava Zang, Zanjan 45137-66731, Iran*

[2]*Bogoliubov Laboratory of Theoretical Physics, Joint Institute for Nuclear Research, Dubna, Moscow Region 141980, Russian Federation*

[3]*Zentrum für Optische Quantentechnologien, Universität Hamburg, Luruper Chaussee 149, 22761 Hamburg, Germany*

(Received 29 October 2012; published 26 December 2012)

We develop and analyze a theoretical model which yields the shifts and widths of Feshbach resonances in an atomic waveguide. It is based on a multichannel approach for confinement-induced resonances (CIRs) and atomic transitions in the waveguides in the multimode regime. In this scheme we replace the single-channel scalar interatomic interaction by the four-channel tensorial potential modeling resonances of broad, narrow, and overlapping character according to the two-channel parametrization of Lange *et al.* [Phys. Rev. A **79**, 013622 (2009)]. As an input the experimentally known parameters of Feshbach resonances in the absence of the waveguide are used. We calculate the shifts and widths of s-, d-, and g-wave magnetic Feshbach resonances of Cs atoms emerging in harmonic waveguides as CIRs and resonant enhancement of the transmission at zeros of the free space scattering length. We have found the linear dependence of the width of the resonance on the longitudinal atomic momentum and quadratic dependence on the waveguide width. Our model opens possibilities for quantitative studies of the scattering processes in ultracold atomic gases in waveguides beyond the framework of s-wave resonant scattering.

DOI: 10.1103/PhysRevA.86.062713 PACS number(s): 34.10.+x, 03.75.Be, 34.50.−s

I. INTRODUCTION

Impressive progress of the physics of ultracold quantum gases has opened new pathways for the study of low-dimensional few-body systems (see, for example [1,2]) as well as strongly correlated many-body systems [3,4]. Specifically, it was shown that the confining geometry of atomic traps can drastically change the scattering properties of ultracold atoms and induce resonances in the collisions [confinement-induced resonances (CIRs)] [5]. The CIR for bosons has been found to occur in the vanishing energy collisional limit as a consequence of the coincidence of the binding energy of a diatomic molecular state with the energy spacing between the levels of the confining (harmonic) potential [6–8]. It was shown that this coincidence leads to a divergence of the effective interatomic coupling constant g_{1D} and to a total atom-atom reflection, which appears as a broad dip in the transmission coefficient T, thereby creating a gas of impenetrable bosons [9]. CIRs have also been extensively studied, e.g., in the context of three-body [10,11] and four-body [12] scattering in confining traps, fermionic p-wave scattering [13], and distinguishable atom scattering [7,14–16] or multichannel scattering [8,17,18] in atomic waveguides. Two novel effects were predicted for distinguishable atoms: the so-called dual CIR yielding a complete suppression of quantum scattering [14], and the resonant molecule formation in tight waveguides [16]. d-wave resonant scattering of bosons in confining harmonic waveguides has been analyzed very recently in Ref. [19]. Coupled l-wave CIRs in cylindrically symmetric waveguides has been studied in Ref. [20]. Remarkable experimental progress has led to the observation of CIRs, for identical bosons [21–24] and fermions [25–27], as well as to distinguishable atoms [28].

However, the recent experimental [24,27–29] and theoretical [17,30–32] investigations of the CIRs clearly show that, despite the impressive progress, the existing theoretical models of CIRs need to be improved for a quantitative description of the experiments in this field. The obvious drawback of the existing theoretical models for CIRs in atomic waveguides is the single-channel character of the simple interatomic interactions employed. Single-channel potentials with zero-energy bound states were used for simulating magnetic Feshbach resonances in free space representing a necessary ingredient for the appearance of the CIR in a confining trap (see, for example, [1,4]). In the seminal work of Olshanii [5] and in subsequent papers [6,33], including the recent works [30,31], the simple form of a pseudopotential was used modeling the interatomic interactions. More realistic potentials were used in our previous works [8,14–17,19] as well as in the works of other authors [6,13,32,34] which, however, all possess a single-channel character. The single-channel interatomic interaction approach permits one to explore only the main attribute of the Feshbach resonances in the three-dimensional free space, namely, the appearance of a singularity in the s-wave scattering length $a_s \to \pm\infty$ when the molecular bound state with energy E_B crosses the atom-atom scattering threshold at energy $E = 0$ in the entrance channel. However, other important parameters of the Feshbach resonance, such as the rotational and spin structure of the molecular bound state in the closed channel as well as the width Δ of the resonance characterizing the coupling Γ of the molecular state with the entrance channel, were ignored. The main goal of the present work is to extend these theoretical approaches developed earlier for the CIRs and transverse excitations and deexcitation processes for collisions in harmonic waveguides [8] to the case of a

*saeidian@iasbs.ac.ir
†melezhik@theor.jinr.ru
‡peter.schmelcher@physnet.uni-hamburg.de

tensorial interaction as well as taking into account the width of the magnetic Feshbach resonances responsible for the CIR. The parameters obtained from the experimental analysis of the magnetic Feshbach resonances in free space, namely, the resonant energies $E_{c,i}$ (or the corresponding values of the field strengths $B_{c,i}$ of the external magnetic field), the widths of the resonances $\Delta_i(\Gamma_i)$, spin characteristics, and the background scattering length $a_{\rm bg}$, are used as input parameters of our model.

It is well known that the most adequate computational schemes including all the above-mentioned parameters of the Feshbach resonances are multichannel scattering [1,35,36] and multichannel quantum-defect [37] approaches providing a quantitative description for a broad regime of experimental parameters for the Feshbach resonances in ultracold atomic gases. In the present work the two-channel potential scheme [36], permitting the efficient modeling of the interatomic interaction near the known magnetic Feshbach resonances of the Cs gas in free space [35], is included in our multichannel approach [8] instead of the simplified interparticle single-channel potential we have used so far for analyzing CIRs and transverse excitations in atomic waveguides. With this approach we model s-, d-, and g-wave Feshbach resonances in ultracold Cs (s, d, and g indicate here the "exit" channels, i.e., they correspond to rotational quantum numbers of the molecular states in the closed channels), which were observed in free space scattering experiments [35], and quantitatively analyze the shifts and widths of the resonances in the harmonic waveguides at experimental conditions closed to the ones encountered in the works [23,24]. We note that selected aspects of the modeling of magnetic Feshbach resonances in optical traps and lattices were also considered in Refs. [38–42].

II. FESHBACH RESONANCE MODEL

We consider the collision of two identical bosonic atoms in a harmonic waveguide. This two-body problem permits the separation of the center-of-mass and relative motion yielding the following Hamiltonian for the relative atomic motion

$$\hat{H}(r,\theta) = \left[-\frac{\hbar^2}{2\mu}\nabla^2 + \frac{1}{2}\mu\omega_\perp^2\rho^2\right]\hat{I} + \hat{V}(r) \qquad (1)$$

with $\rho = r\ \sin\ \theta$ and the trap potential $1/2\mu\omega_\perp^2\rho^2$. $\hat{V}(r)$ is the four-channel interatomic potential, $\hat{I}$ is the unit matrix, r is the relative radial coordinate, and $\mu = m/2$ is the reduced mass of the atoms.

Following the scheme suggested in Ref. [36] for describing the three magnetic Feshbach resonances in an ultracold Cs gas, let us suppose that initially the scattering atoms are prepared in one spin configuration $|e\rangle$ (called the "entrance channel") and the "closed channels" $|c,i\rangle$ ($i = 1, 2, 3$) support s-, d-, and g-wave molecular bound states at -11.1, 47.78, and 53.449 G, respectively. The quantum state of an atomic pair with energy E is described as

$$|\psi\rangle = \sum_{i=1}^{3}\psi_{c,i}(\mathbf{r})|c,i\rangle + \psi_e(\mathbf{r})|e\rangle$$

satisfying the Schrödinger equation with the Hamiltonian (1). A four-channel square-well potential

$$\hat{V} = \begin{pmatrix} -V_{c,3} & 0 & 0 & \hbar\Omega_3 \\ 0 & -V_{c,2} & 0 & \hbar\Omega_2 \\ 0 & 0 & -V_{c,1} & \hbar\Omega_1 \\ \hbar\Omega_3 & \hbar\Omega_2 & \hbar\Omega_1 & -V_e \end{pmatrix} \text{(if } r < \overline{a}\text{)}$$

$$= \begin{pmatrix} \infty & 0 & 0 & 0 \\ 0 & \infty & 0 & 0 \\ 0 & 0 & \infty & 0 \\ 0 & 0 & 0 & 0 \end{pmatrix} \text{(if } r > \overline{a}\text{)} \qquad (2)$$

is employed to describe the colliding atoms in the "entrance channel" $|e\rangle$ and the weakly bound molecules in the "closed channels" $|c,i\rangle$ near a Feshbach resonance. For $r < \overline{a} = 4\pi\Gamma(1/4)^{-2}R_{\rm vdW}$, we assume the attractive potential can support multiple molecular states—that is, $V_e, V_{c_i} \gg E_{\rm vdW} = \hbar^2/2\mu R_{\rm vdW}^2$—and $\hbar\Omega_i$ induce Feshbach couplings between the channels [36]. The size $\overline{a}$ of the potential action is chosen to account for the interatomic interaction determined by the van der Waals (vdW) tail with the length $R_{\rm vdW} = 1/2(2\mu C_6/\hbar^2)^{1/4}$ and the energy scale $E_{\rm vdW} = \hbar^2/2\mu R_{\rm vdW}^2$ [43], where C_6 is the corresponding van der Waals coefficient and $\Gamma(x)$ is the Γ function. For $r > \overline{a}$, entrance- and closed-channel thresholds are set to be $E = 0$ and $E = \infty$, respectively (see Fig. 1 in Ref. [36]).

Such a choice of the interatomic interaction permits a simple parametrization of the atom-atom scattering in universal terms of the energy of the ith bare bound state E_i, the Feshbach coupling strength of the bound molecular state with the entrance channel Γ_i, and the background scattering length $a_{\rm bg}$, which is convenient for an analysis of experimental data near magnetic Feshbach resonances [1,36]. When the mixing between the closed channels and the entrance channel is weak and the background scattering length $|a_{\rm bg}|$ considerably exceeds the range of the interatomic interaction $\overline{a}$, the s-wave scattering length a and the binding energy E_b in free space are given by [36]

$$\frac{1}{a-\overline{a}} = \frac{1}{a_{\rm bg}-\overline{a}} + \frac{1}{\overline{a}}\sum_{i=1}^{3}\frac{\Gamma_i/2}{E_i} \qquad (3)$$

and

$$E_b = \frac{\hbar^2 k_m^2}{2\mu}, \quad k_m = \frac{1}{a_{\rm bg}-\overline{a}} + \frac{1}{\overline{a}}\sum_{i=1}^{3}\frac{\Gamma_i/2}{E_b+E_i}, \qquad (4)$$

respectively. Then, assuming that the bare bound states can be linearly tuned magnetically by a linear Zeeman shift—namely, $E_i = \delta\mu_i(B - B_{c,i})$, where $\delta\mu_i$ is the relative magnetic moment between the entrance and ith channels and $B_{c,i}$ is the crossing field value of the ith bare bound state, the scattering length $a(B)$ can be represented as

$$\frac{a}{a_{\rm bg}} = \prod_{i=1}^{3}\frac{B-B_i^*}{B-B_{0,i}}. \qquad (5)$$

Here $B_{0,i}$ is the ith lowest pole of a and B_i^* is the ith lowest zero. The width of the ith Feshbach resonance can be defined as $\Delta_i = B_i^* - B_{0,i}$. The binding energy of Feshbach molecules

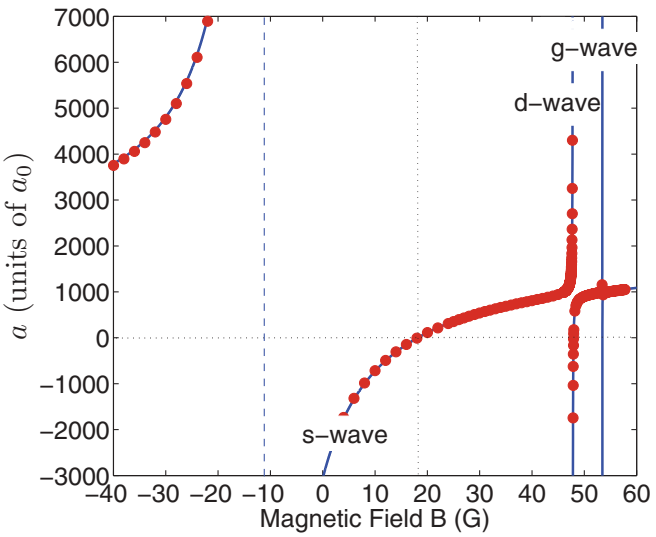

FIG. 1. (Color online) The s-wave scattering length a of $|F = 3, m_F = 3\rangle$ Cesium atoms as a function of the magnetic field B. The solid curve shows the analytical result (5) and the dots show the numerical result (see the text).

can be measured in the experiment by, e.g., radio frequency and microwave spectroscopy [44–48]. Using the fitting parameters $a_{\rm bg}$, $\delta\mu_i$, Γ_i, and $B_{c,i}$, one can fit the experimental data [44–48] with (4), from which one can calculate $a(B)$ (3), B_i^*, and $B_{0,i}$ (5) [36].

The result of the procedure is given in the Table I of Ref. [36] for ultracold Cs Feshbach molecules where $a_{\rm bg} = 1875a_0$ and $\overline{a} = 95.7a_0$ (a_0 is the Bohr radius) are also given. With these values for $B_{0,i}$ and B_i^* we show the scattering length $a(B)$ as a function of the magnetic field B according to Eq. (5), in Fig. 1.

The parameters $a_{\rm bg}$, $\delta\mu_i$, Γ_i, $B_{c,i}$, B_i^*, and $B_{0,i}$ from [36] together with $a(B)$ defined by Eq. (5) are used for fitting the diagonal terms $V_{c,i}$ and V_e in the tensor potential (2). The nondiagonal terms $\hbar\Omega_i$ are defined by the formulas [36]

$$\Gamma_i/2 = 2\theta^2 V_{c,i}, \quad \tan 2\theta_i = \frac{2\hbar\Omega_i}{V_e - V_{c,i}}.$$

The scattering length $a(B)$ is then calculated for different B and varying parameters of the potential $\hat{V}$ by solving the Schrödinger equation

$$\left(\left[-\frac{\hbar^2}{2\mu}\nabla^2 + \frac{1}{2}\mu\omega_\perp^2\rho^2\right]\hat{I} + \hat{B} + \hat{V}(r)\right)|\psi\rangle = E|\psi\rangle \qquad (6)$$

in free space ($\omega_\perp = 0$) with the scattering boundary conditions

$$\psi_e(\mathbf{r}) \to \exp\{ikz\} + f(k,\theta)/r\,\exp\{ikr\}, \qquad \psi_{c,i}(\mathbf{r}) \to 0$$

at $kr \to \infty$ for the fixed $E \to 0$ ($k = \sqrt{2\mu E}/\hbar \to 0$) [49]. The diagonal matrix $\hat{B}$ in Eq. (6) is defined as $B_{ii} = \delta\mu_i(B - B_i)$ ($i = 1,2,3$) and $B_{ee} = 0$. After separation of the angular part in Eq. (6) we come to the system of four coupled radial equations

$$\left[-\frac{\hbar^2}{2\mu}\frac{d^2}{dr^2} + \frac{\hbar^2 l_\alpha(l_\alpha+1)}{2\mu r^2} + B_{\alpha\alpha}\right]\phi_\alpha(r) + \sum_\beta V_{\alpha\beta}(r)\phi_\beta(r) = E\phi_\alpha(r) \qquad (7)$$

for the radial part $\phi_\alpha(r)$ of the desired wave function $|\psi\rangle = \sum_\alpha \psi_\alpha(\mathbf{r})|\alpha\rangle = \sum_\alpha \phi_\alpha(r)Y_{l_\alpha 0}(\hat{r})|\alpha\rangle$, where $\alpha = \{e,i = 1,2,3\}$ ($l_e = 0$, $l_1 = 0$, $l_2 = 2$, $l_3 = 4$) and the matrix elements $V_{\alpha\beta}(r)$ are defined by Eq. (2). The centrifugal barrier $+\frac{\hbar^2 l_\alpha(l_\alpha+1)}{2\mu r^2}$ in Eq. (7) models at $r \to 0$ the correct asymptotic behavior $\phi_i(r) \sim r^{l_i+1}$ of the molecular bound states $|c,i\rangle$ in the closed channels which couple to the entrance s-wave ($l_e = 0$) channel $|e\rangle$ by the nondiagonal terms $V_{\alpha\beta}(r)$ ($\alpha \neq \beta$).

By varying the $V_{c,i}$, V_e, and Ω_i we obtain an excellent agreement of the calculated s-wave scattering length $a(B)$ with the analytical results from [36] for cesium atoms in the hyperfine state $|F = 3, m_F = 3\rangle$ for the considered magnetic field regime -40 G $< B <$ 60 G (see dots in Fig. 1). In this regime, we observe three resonance terms, which correspond to the coupling to the s-, d-, and g-wave molecular states.

Next we analyze the scattering properties of the s-, d-, and g-wave magnetic Feshbach resonances in harmonic waveguides by integrating the Schrödinger equation (6) for $\omega_\perp \neq 0$ with the scattering boundary conditions

$$\psi_e(\mathbf{r}) = [\cos(k_0 z) + f_e\exp\{ik_0|z|\}]\Phi_0(\rho), \quad \psi_{c,i}(\mathbf{r}) \to 0 \qquad (8)$$

at $|z| = |r\,\cos\,\theta| \to \infty$ adopted for a confining trap [8]. $f_e(E)$ is the scattering amplitude, corresponding to the symmetry with respect to the exchange $z \to -z$ (we consider collisions of identical bosonic Cs atoms), $\Phi_0(\rho)$ is the wave function of the ground state of the two-dimensional (2D) harmonic oscillator, and $k_0 = \sqrt{2\mu(E - \hbar\omega_\perp)}/\hbar = \sqrt{2\mu E_\parallel}/\hbar$. In the presence of the harmonic trap ($\omega_\perp \neq 0$) the problem (6), (8) becomes nonseparable in the plane $\{\rho,z\}$, i.e., the azimuthal angular part is separated in the wave function $|\psi\rangle$ and Eq. (6) is reduced to the coupled system of four 2D Schrödinger-type equations. To integrate this coupled channel 2D scattering problem in the plane $\{r,\theta\}$ we have extended the computational scheme [8].

The computations have been performed in a range of variation of $\omega_\perp$ close to the experimental values of the trap frequencies $\sim 2\pi \times 14.5$ kHz [24]. We have integrated Eq. (6) for varying B and fixed longitudinal colliding energy $E_{||} = E - \hbar\omega_\perp$. In the main part of computations the energy $E_{||}$ was chosen very low $E_{||} = 1.0 \times 10^{-16}(\frac{\hbar^2}{\mu\overline{a}^2}) \to 0$ [$k_0 = 1.0 \times 10^{-8}(\frac{1}{a_0}) \to 0$] to have a possibility for direct comparison with existing pseudopotential estimates obtained in zero-energy limit. The integration was performed in the units of the problem leading to the scale transformation: $r \to \frac{r}{\overline{a}}$, $E \to \frac{E}{E_0}$, $V \to \frac{V}{E_0}$, and $\omega_\perp \to \frac{\omega_\perp}{\omega_0}$ with $E_0 = \frac{\hbar^2}{\mu\overline{a}^2}$ and $\omega_0 = \frac{E_0}{\hbar}$.

III. RESULTS AND DISCUSSION

A. Transmission coefficient

In Fig. 2 we present the transmission coefficient $T(B) = |1 + f_e(B)|^2$ as a function of B calculated for the harmonic trap $\omega_\perp = 14.9$ kHz with the two-channel ($i = 1$) and four-channel ($i = 1,2,3$) character of the tensorial interaction $\hat{V}(r)$ (2). The two-channel potential $\hat{V}(i = 1)$ supports only one broad s-wave Feshbach resonance, while the four-channel

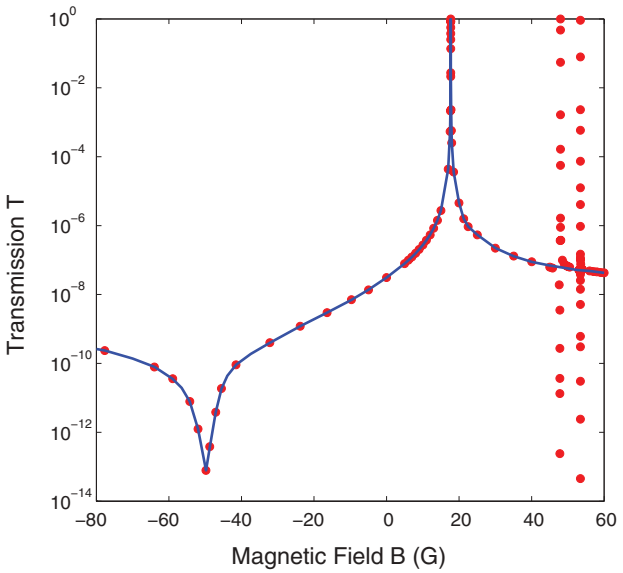

FIG. 2. (Color online) The transmission coefficient T for the harmonic trap with $\omega_\perp = 14.9$ kHz as a function of the magnetic field B for the case of the two-channel (solid curve) and four-channel (dots) potential (2).

potential $\hat{V}(i = 1,2,3)$ supports all three s-, d-, and g-wave magnetic Feshbach resonances in free space ($\omega_\perp = 0$) at the fields $B_{0,1} = -11.1$ G, $B_{0,2} = 47.78$ G, and $B_{0,3} = 53.449$ G, respectively [36]. All these resonances are also developed in the calculated curve $T(B)$ of the transmission coefficient in the trap ($\omega_\perp \neq 0$).

First, we have analyzed the region of $B \simeq -11.1$ G near the s-wave resonance. In Fig. 3 we show the calculated 1D

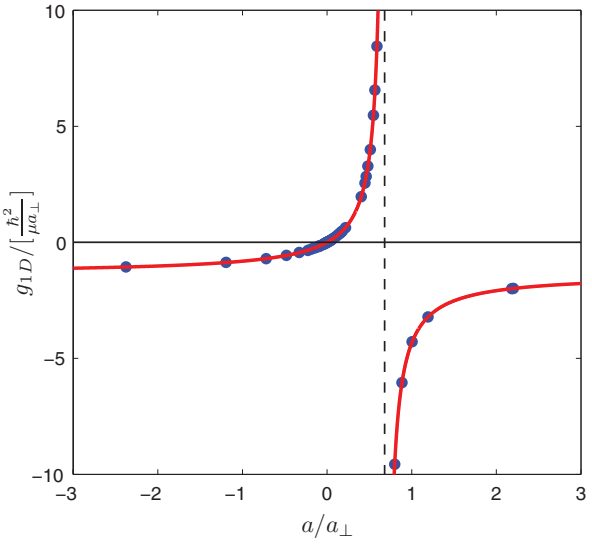

FIG. 3. (Color online) The coupling constant g_{1D} as a function of the scattering length a in free space in the region near the s-wave Feshbach resonance, calculated for the harmonic trap with $\omega_\perp = 14.9$ kHz. Dots indicate the numerical data and the solid curve the analytical results with the formulas derived in the pseudopotential approach [5].

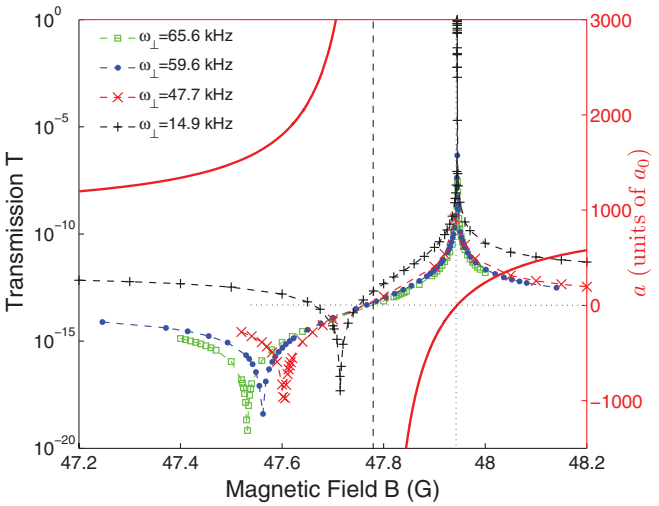

FIG. 4. (Color online) The transmission coefficient $T(B)$ as a function of the strength of the magnetic field for several trap frequencies $\omega_\perp$. Here the s-wave scattering length $a(B)$ from Fig. 1 is also given (solid line).

coupling constant $g_{1D} = \lim_{k_0 \to 0} \mathrm{Re}\{f_e(k_0)\}/\mathrm{Im}\{f_e(k_0)\}k_0/\mu$ [6] as a function of the scattering length $a(B)$ in this region. By tuning B in the interval -60 G $\leqslant B \leqslant 40$ G, the s-wave scattering length $a(B)$ changes from $-\infty$ to $+\infty$. At $B = -49.78$ G corresponding to the point $a(B) = a_\perp/C$ (where $C = 1.4603$ and $a_\perp = \sqrt{\hbar/\mu\omega_\perp}$) of the appearance of the CIR [5], the coupling constant $g_{1D}(a/a_\perp)$ diverges and the behavior is in very good agreement with our previous computation of $g_{1D}(a/a_\perp)$ performed with the single-channel screened Coulomb potential [8] and the formulas $g_{1D} = 2\hbar a/(\mu a_\perp^2)/(1 - Ca/a_\perp)$ derived in a pseudopotential approach [5].

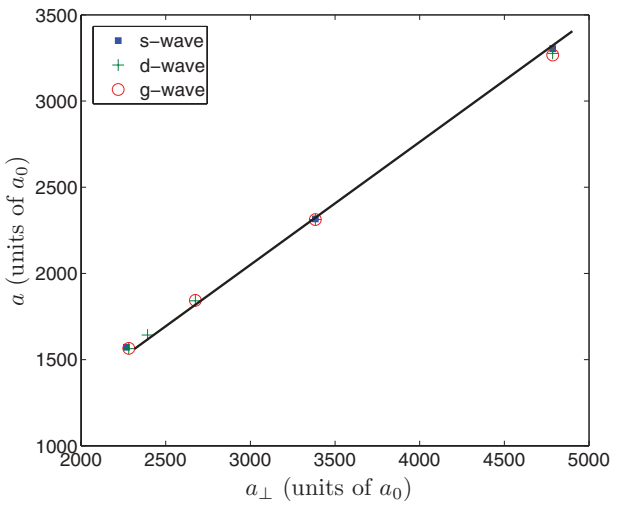

FIG. 5. (Color online) The dependence of the s-wave scattering length $a(B)$ on the width $a_\perp$ of the waveguide at the points $B_{\min}$ of the minimum of the transmission coefficient $T(a(B),a_\perp)$ (see Fig. 4). The dots, pluses, and circles correspond to the calculated points near the s-, d-, and g-wave magnetic Feshbach resonances, respectively. The solid curve corresponds to the formula $a = a_\perp/C$ [5].

Let us next analyze the region of the d-wave magnetic Feshbach resonance near the point 47.78 G (see Fig. 1)—the region of major experimental interest due to atomic loss and the formation of Cs molecules in the confined ultracold gas of Cs atoms [23,24]. The results of our computations are illustrated by the curves $T(B)$ calculated for different $\omega_\perp$ (Fig. 4) corresponding to the transverse frequencies of the optical trap being used in the experiment [24]. It is clearly shown that the position $B_{\min}$ of the transmission coefficient $T(B)$ minimum is dependent on the trap width $a_\perp = \sqrt{\hbar/(\mu\omega_\perp)}$ and the corresponding scattering length $a(B_{\min})$ at the point $B_{\min}$ is accurately described by the formulas $a(B_{\min}) = a_\perp/C$ obtained by Olshanii [5] for the position of the CIR in a harmonic waveguide. The latter fact is illustrated in Fig. 5. Here the results of the calculation of the dependence of $a(B_{\min})$ on $a_\perp$ for s-wave and g-wave Feshbach resonances are also given. This analysis clearly demonstrates that the law $a = a_\perp/C$ for the position of the CIR in a harmonic waveguide is fulfilled with high accuracy for the Feshbach resonances of different tensorial structure, although the law was initially obtained at zero-energy limit in the framework of an s-wave single-channel pseudopotential approach to the interatomic interaction [5]. We also see that the positions $B_{\max}$ of the maximums of the coefficients $T(B)$ calculated for different $\omega_\perp$ are independent of $\omega_\perp$ and coincide at the point $B_2^* = 47.944$ G of the zero of the scattering length in free space $[a(B_2^*) = 0]$. This fact is in agreement with the analytic result $T = |1 + f_e|^2 \to 1$ obtained in the pseudopotential approach at $a \to 0$. The same behavior of the $T(B)$ coefficients has been found in the vicinity of 18.1 and 53.46 G (points B_1^* and B_3^* of s-wave scattering length zeros near the s- and g-wave Feshbach resonances).

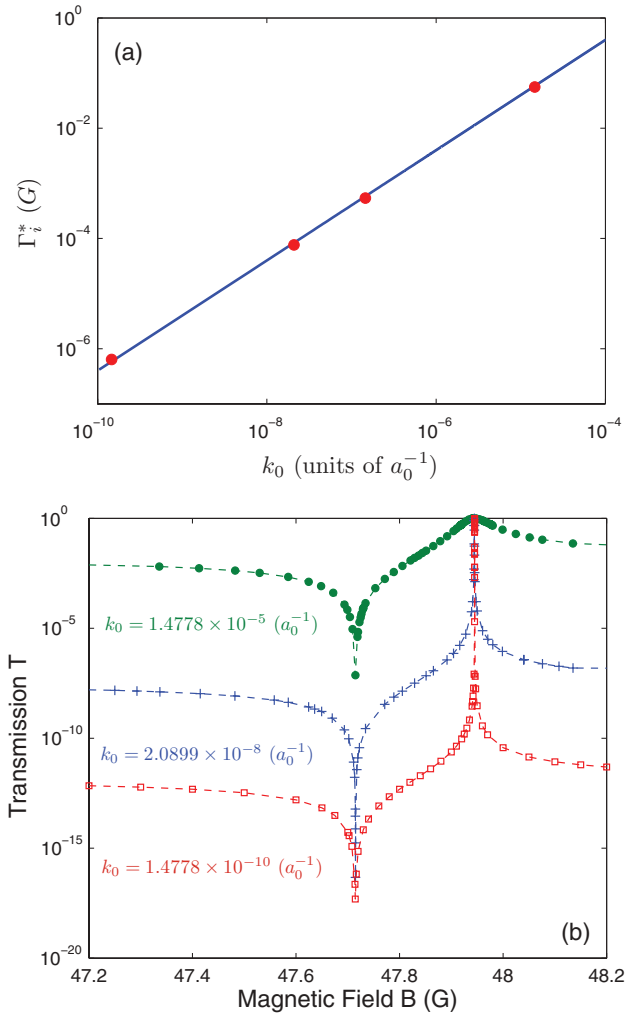

FIG. 6. (Color online) (a) The dependence of the width Γ_i^* on the longitudinal momentum k_0 near the d-wave Feshbach resonance. The solid line has been obtained via Eq. (10); solid circles indicate the widths $\Gamma_i^*(k_0)$ extracted from the numerically calculated $T(B,k_0)$. (b) The transmission coefficient T as a function of the magnetic field B calculated for a few k_0. For both subfigures $\omega_\perp = 14.9$ kHz.

B. Width of the resonant enhancement of the transmission

While the coefficients $T(B)$ in the vicinity of the points B_i^* [positions of the zeros of the scattering length $a(B)$] show a resonant behavior one can define the width Γ_i^* of this resonance as the width at half T maximum. By using the formulas for the even scattering amplitude in the trap [18,50]

$$f_e = -\frac{1}{1 + i\,\cot\,\delta_{1D}} = -\frac{1}{1 + ik_0 a_{1D}}$$

valid near the CIR in the zero-energy limit and the definitions $a_{1D} = \frac{a_\perp}{2}(C - \frac{a_\perp}{a})$ and $a = a_{bg}\prod_{i=1}^{3}\frac{(B-B_i^*)}{(B-B_{0,i})}$, we obtain

$$\Gamma_i^* = \frac{4a_{bg}\gamma_i a_\perp^2 k_0 \Delta_i}{4a_{bg}^2\gamma_i^2 - a_\perp^4 k_0^2\left(1 - C\gamma_i\frac{a_{bg}}{a_\perp}\right)^2}, \tag{9}$$

where $\gamma_i = \prod_{j\neq i}^{3}\frac{(B_i^*-B_j^*)}{(B_i^*-B_{0,j})}$. The above formula is valid for the condition $\Gamma_i^* \ll B_i^*$ of narrow resonances, which is fulfilled with high accuracy for the d- and g-wave resonances and less

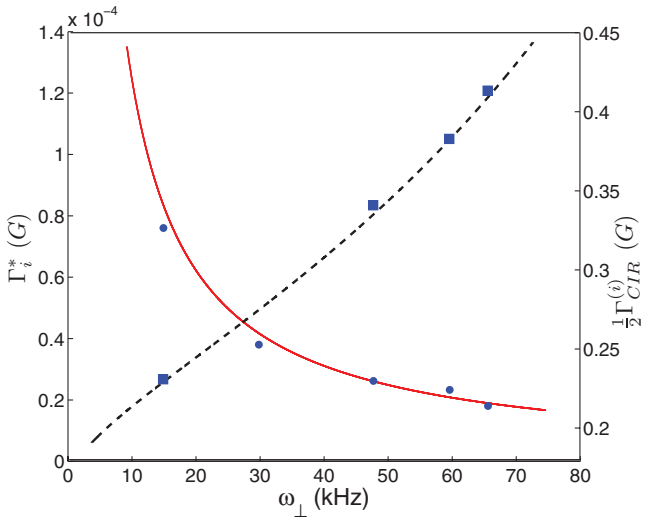

FIG. 7. (Color online) The dependence of the width Γ_i^* on the trap frequency $\omega_\perp$ near the d-wave Feshbach resonance at $k_0 = 2.0899 \times 10^{-8}(a_0^{-1})$. The solid curve has been obtained via Eq. (10); solid circles indicate the widths $\Gamma_i^*(\omega_\perp)$ extracted from the numerically calculated $T(B,\omega_\perp)$. The analytical (dashed line) and numerical (squares) results for the right half-width $1/2\Gamma_{CIR}^{(i)}$ versus $\omega_\perp$ are also given.

accurately for s-wave resonance (see Fig. 2). In the low energy limit $k_0 \to 0$ the expression is reduced to

$$\Gamma_i^* = \Delta_i \frac{a_\perp^2 k_0}{a_{\rm bg}\gamma_i} = \Delta_i \frac{\sqrt{2E_\parallel}}{\sqrt{\mu} a_{\rm bg}\omega_\perp \gamma_i}, \tag{10}$$

where $\Delta_i = B_i^* - B_{0,i}$ is the width of the Feshbach resonance in free space and the dimensionless γ_i factor $\approx \frac{1}{2}$ for the case of d- and g-wave resonances and ≈ 1 for the s-wave resonance. Figures 6 and 7 demonstrate the very good agreement of these formulas with the numerical computations. Actually, in Fig. 6(a) one can see in a broad range of k_0 variation the very good agreement of the width $\Gamma_i^*(k_0)$, extracted from numerically calculated $T(B,k_0)$, with the linear functional dependence on the longitudinal momentum k_0, following from Eq. (10). Also, the $\Gamma_i^*(\omega_\perp)$ has inverse dependence on $\omega_\perp$. It is confirmed by the results of the numerical calculations of $\Gamma_i^*(\omega_\perp)$ given in Fig. 7. Thus, Eq. (10) can be used for extracting important information about the analyzed system.

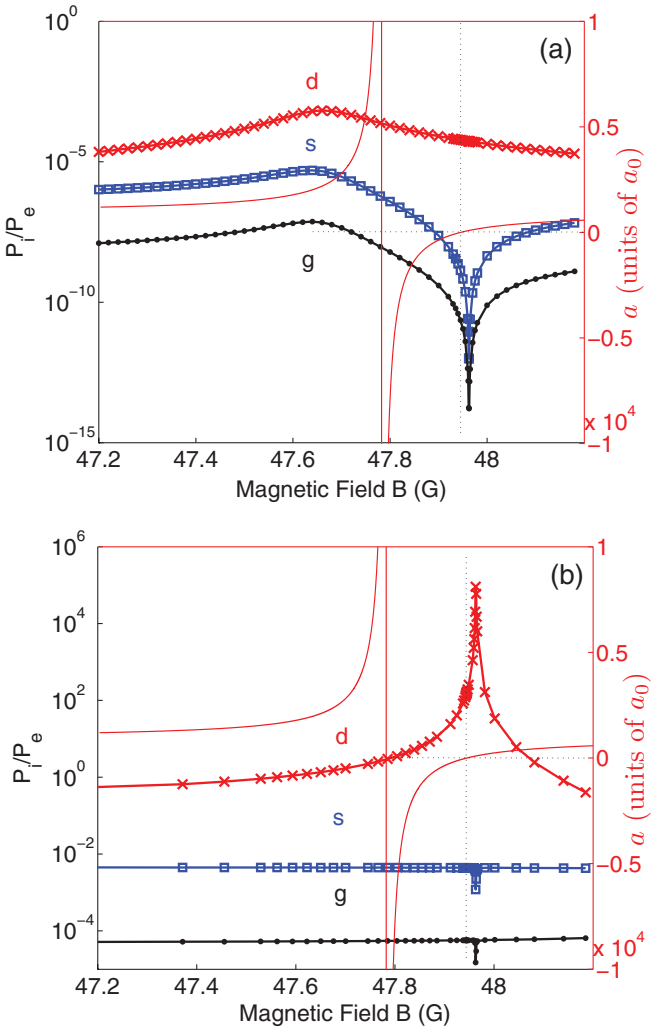

FIG. 8. (Color online) The relative populations P_i/P_e (13) of the molecular states $i = s$, d, and g calculated as a function of B near the d-wave Feshbach resonance in Cs for the pair collisions in free space (a) and in the harmonic waveguide with $\omega_\perp = 59.6$ kHz (b). The s-wave scattering length $a(B)$ in free space from Fig. 1 is also given.

Indeed, by measuring the width Γ_i^* one can extract from Eq. (10) the longitudinal momentum $k_0 = \sqrt{2\mu E_\parallel}/\hbar$ (longitudinal colliding energy $E_\parallel$) and estimate the "longitudinal" temperature of the atomic cloud in the trap. This expression also shows that one can control the width Γ_i^* of the resonance by varying the trap frequency $\omega_\perp$. Increasing $\omega_\perp$ leads to a narrowing of the resonance (see Figs. 4 and 7), the effect of which can be used experimentally. Figure 6(b) demonstrates the stability of the position of the CIR (the minimum of the transmission coefficient T) with respect to k_0 variation and the linear growth of the transmission coefficient T with increasing k_0. It is shown that already at very low $k_0 \sim 10^{-5}(\frac{1}{a_0})$ the T coefficient becomes large enough and consequently can be experimentally "visible" near CIR.

To conclude this section we also give the expression for the position of the CIR with respect to the resonance at $a = 0$ (to the point B_i^*):

$$\Delta_{\rm CIR}^{(i)} = \frac{\Delta_i}{1 - C\gamma_i \frac{a_{\rm bg}}{a_\perp}}. \tag{11}$$

Since the resonance maximum at B_i^* corresponds to the unit value $T(B_i^*) \to 1$ and the minimum of the CIR approaches zero $T(B_i^* - \Delta_{\rm CIR}^{(i)}) \to 0$, we can define the "right" half-width $\frac{1}{2}\Gamma_{\rm CIR}^{(i)}$ of the CIR as the distance of the zero of the coefficient T to the right situated point where $T = \frac{1}{2}$. Using the formulas for $\Delta_{\rm CIR}^{(i)}$ and Eq. (10) for Γ_i^* we obtain

$$\frac{1}{2}\Gamma_{\rm CIR}^{(i)} = \Delta_{\rm CIR}^{(i)} - \frac{1}{2}\Gamma_i^* \xrightarrow[(k_0 \to 0)]{} \Delta_i \left[\frac{1}{1 - C\gamma_i \frac{a_{\rm bg}}{a_\perp}} - \frac{a_\perp^2 k_0}{2 a_{\rm bg}\gamma_i} \right]. \tag{12}$$

The above expression describes the narrowing of the CIR width $\Gamma_{\rm CIR}^{(i)}$ with decreasing trap frequency $\omega_\perp$, opposite to Γ_i^* (see Fig. 4). This expression might also be of interest to the experimental analysis of the CIRs.

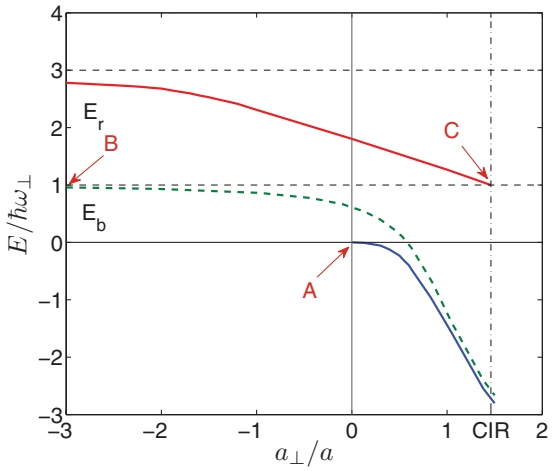

FIG. 9. (Color online) Schematic picture (presented in Refs. [6, 17] for a single-channel potential model of interatomic interaction) of the bound state energy E_b of two atoms as a function of $a_\perp/a$ in free space (solid line) and in the harmonic waveguide (dashed line). The first excited resonance state energy E_r is also presented.

C. Population of molecular states in free space and in the waveguide

We have also calculated the relative populations P_i/P_e of the molecular states $|c,i\rangle$ in the process of pair atomic collisions for harmonic traps of different frequencies $\omega_\perp$ as well as in free space ($\omega_\perp = 0$). The populations P_i are defined as

$$P_i = 2\pi \int_0^\infty \int_0^\pi |\psi_{c,i}(r,\theta)|^2 r^2 dr \, \sin\theta \, d\theta, \qquad (13)$$

where integration over the infinite region $0 \leqslant r < \infty$ gives a convergent result due to the decaying tails of the molecular bound-state wave functions $\psi_{c,i}(\mathbf{r}) \to 0$ at distances of the order $\sim\bar{a}$ in the closed channels $|c,i\rangle$. The population P_e is defined in a region near the origin $r \to 0$ of the molecular dimension $\sim\bar{a}$ in the entrance channel by using Eq. (13) where the upper limit of the integration over r is $\bar{a}$. The relative populations P_i/P_e of the molecular states for ultracold atomic collisions in free space and in the harmonic waveguide with $\omega_\perp = 59.6$ kHz are shown in Fig. 8 in the region of B near the d-wave Feshbach resonance. In free space the pair collision leads to a relatively low population of the d-wave molecular state $P_2/P_e \sim 10^{-4}$–10^{-5}. The populations of nonresonant s- and g-wave states are $P_1 \ll P_2$ and $P_3 \ll P_2$ essentially suppressed here. The dependence of the d-wave molecular state population on B repeats the dependence on B of the population of the region $\sim\bar{a}$ in the entrance channel $P_2(B)/P_e(B) \sim$ const. However, in the confined geometry of the waveguide ($\omega_\perp \neq 0$) the pair collision leads to a resonant enhancement of the relative population $P_2(B)/P_e(B)$ of the d-wave molecular state near the point $B_2^* = 47.944$ G where the free space scattering length is zero $a(B_2^*) = 0$. In the waveguide the point of appearance of the bound state is shifted from the position defined by $1/|a| \to 0$ for free space scattering (see point A in the illustrative scheme of the bound and resonant states of an atomic pair given in Fig. 9) to the point $1/|a| \to \infty$ (the point B in Fig. 9). This is why we observe in Fig. 8(b) the strong resonant enhancement of the

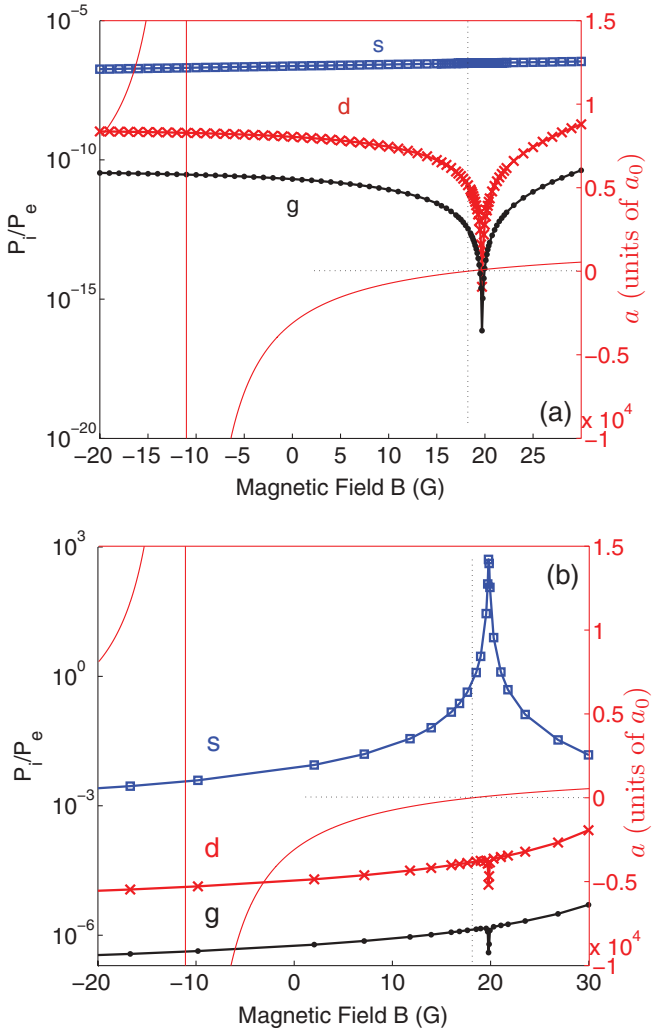

FIG. 10. (Color online) The relative populations P_i/P_e (13) of the molecular states $i = s$, d, and g calculated as functions of B near the s-wave Feshbach resonance for Cs for the pair collisions in free space (a) and in the harmonic waveguide with $\omega_\perp = 59.6$ kHz (b). The s-wave scattering length $a(B)$ from Fig. 1 is also presented.

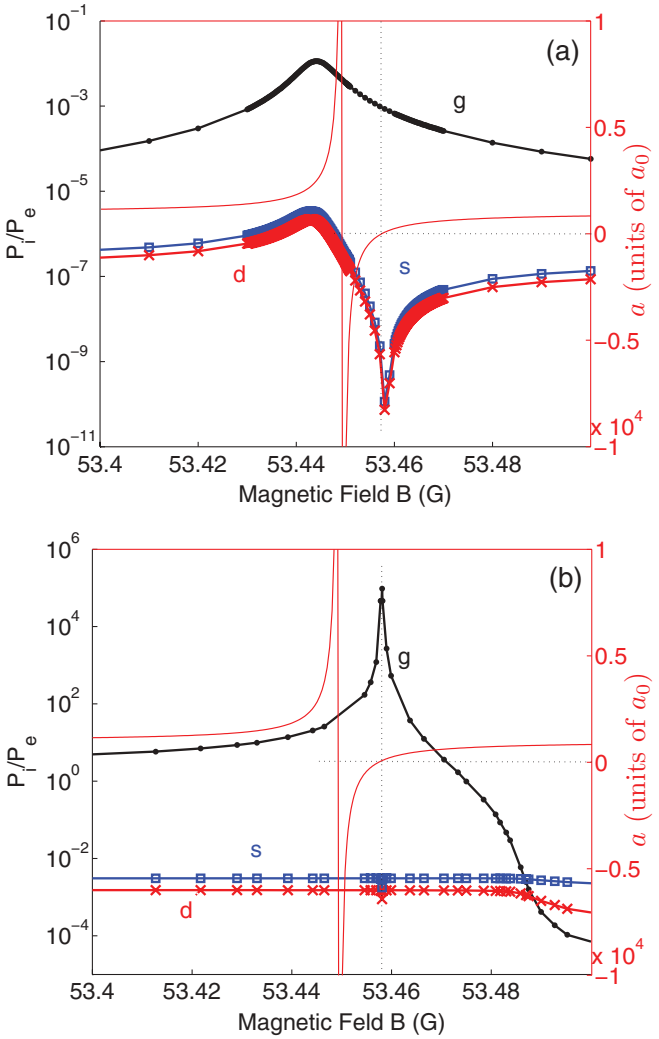

FIG. 11. (Color online) The relative populations P_i/P_e (13) of the molecular states $i = s$, d, and g calculated as functions of B near the g-wave Feshbach resonance in Cs for the pair collisions in free space (a) and in the harmonic waveguide with $\omega_\perp = 59.6$ kHz (b). The s-wave scattering length $a(B)$ from Fig. 1 is also presented.

population $P_2(B_2^*)$ at the magnetic field $B_2^* = 47.944$ G. The populations P_1/P_e and P_3/P_e of other molecular states also show some enhancement with respect to the entrance channel due to the coupling of the states with the "resonance" channel $|c,2\rangle$, which, however, are a few orders of magnitude less than the enhancement of the population P_2/P_e. We do not observe a resonant behavior of $P_2(B)$ at the point $B = 47.57$ G of the CIR (see Fig. 4 and the point C in Fig. 9). We suspect that this is the case due to the rather weak coupling in our model potential $\hat{V}(2)$ between the entrance channel $|e\rangle$ and the resonant state in the closed channel $|c,2\rangle$ for stimulating considerable transition to the molecular state $|c,2\rangle$ in the closed excited channel of the waveguide.

In Figs. 10 and 11 we present the results of our computation of the molecular state populations near the s- and g-wave Feshbach resonances -11.1 G and 53.449 G, respectively. We observe the qualitatively analogous effect of resonant enhancement of the relative populations $P_1(B)/P_e(B)$ and $P_3(B)/P_e(B)$ at the points $B_1^* = 18.1$ G and $B_3^* = 53.457$ G in the harmonic waveguide, which correspond to the positions of the zero of the s-wave scattering length in the vicinity of s- and g-wave Feshbach resonances, respectively. Here we notice $P_1(B)/P_e(B) \simeq$ const, i.e., the same dependence on B of the s-wave molecular state population as the population of the region $\leqslant \bar{a}$ in the entrance channel [see Fig. 10(a)]. In Fig. 11(a) we observe the resonant enhancement of the relative population $P_3(B)/P_e(B)$ of the g-wave molecular state near the Feshbach resonance in free space at $B_{0,3} = 53.449$ G, where $1/|a| \to 0$. A similar resonance enhancement near the point $1/|a| \to 0$ of the appearance of the near threshold resonance or weakly bound state in free space (see point A in Fig. 9) is observable via the values $P_1(B)$, $P_2(B)$, and $P_e(B)$ but, because $P_1(B)/P_e(B) \simeq$ const and $P_2(B)/P_e(B) \sim$ const, we do not observe this effect in the relative populations $P_1(B)/P_e(B)$ and $P_2(B)/P_e(B)$ in Figs. 10(a) and 8(a).

IV. CONCLUSION

We have developed a theoretical model for a quantitative analysis of the Feshbach resonance shift and width induced by an atomic waveguide. It is based on our multichannel approach for confinement-induced resonances and atomic transitions in the waveguides in the multimode regime [8]. In this scheme the single-channel (scalar) interatomic interaction is replaced by a four-channel (tensorial) potential modeling resonances of different structure according to the two-channel parametrization of Lange *et al.* [36]. The experimentally known parameters of the Feshbach resonance in the absence of the waveguide are used as an input in our approach. We have calculated the shifts and widths of s-, d-, and g-wave magnetic Feshbach resonances of Cs atoms emerging in harmonic waveguides as CIRs and resonant enhancement of the transmission at zeros of the free space scattering length.

In particular, we find that the relationship $a = a_\perp/C$ for the position of the CIR in a harmonic waveguide is fulfilled with high accuracy for the Feshbach resonances of different tensorial structure which holds in spite of the fact that this property was originally obtained in the framework of an s-wave single-channel pseudopotential approach [5]. Note, that this property was experimentally confirmed for d-wave Feshbach resonances in a gas of Cs atoms [24]. The maximum of the transmission, corresponding to the zero of the scattering amplitude, is shown to be independent of the trap field strength and then again corresponds to the zero B_i^* of the s-wave scattering length $a(B)$ in free space. In a nutshell, the Feshbach resonance in free space develops in the harmonic waveguide into a minimum of T (position of CIR), defined by the formulas $a = a_\perp/C$, and a maximum, coinciding with the position of zero of the s-wave scattering length a. The "distance" between these extrema is equal to $\Delta_{\rm CIR}^{(i)} = \Delta_i/(1 - C\gamma_i a_{\rm bg}/a_\perp)$.

We have derived expressions for the widths $\Gamma_i^*, \frac{1}{2}\Gamma_{\rm CIR}^{(i)}$ of the resonant enhancement of T at B_i^* and the "right" side half-width of the minimum of the T coefficient, i.e., at the position of CIR, and confirmed its validity by numerical results for $k_0 \to 0$. By measuring the width Γ_i^* one can, in principle, extract from these expressions the longitudinal collision energy and estimate the "longitudinal" temperature of the atomic cloud in the trap. In other words the width of the atomic loss resonance observed in the experiment [24] at the point of CIR might contain important information about the longitudinal atomic momentum k_0 and the temperature of the gas. It also shows that one can control the width Γ_i^* of the resonance at $a(B_i^*) = 0$ by varying the trap frequency $\omega_\perp$. An increase of $\omega_\perp$ leads to a narrowing of the resonance, an effect which could potentially be used experimentally.

Finally, the molecule formation rates in a waveguide show an enhancement for the case of a corresponding zero of the s-wave scattering length $a(B_i^*) = 0$. We have shown that the positions of these resonances are stable with respect to the variation of the confining frequency $\omega_\perp$ of the waveguide.

Our model adds to the possible studies of scattering processes of ultracold atomic gases in waveguides beyond the framework of s-wave resonant scattering. Our model might be extended to the cases of fermions or distinguishable atom scattering, including transverse excitation and deexcitation processes [8]. It also permits investigation of other trap geometries [49] and more realistic interatomic interactions.

ACKNOWLEDGMENTS

We thank E. Haller and H.-C. Nägerl for fruitful discussions. V.S.M. and P.S. acknowledge financial support by the Deutsche Forschungsgemeinschaft and the Heisenberg-Landau Program. V.S.M. thanks the Zentrum für Optische Quantentechnologien of the University of Hamburg and Sh.S. thanks the Bogoliubov Laboratory of Theoretical Physics of JINR at Dubna for their warm hospitality.

[1] C. Chin, R. Grimm, P. S. Julienne, and E. Tiesinga, Rev. Mod. Phys. **82**, 1225 (2010).

[2] T. Köhler, K. Góral, and P. S. Julienne, Rev. Mod. Phys. **78**, 1311 (2006).

[3] I. Bloch, J. Dalibard, and W. Zwerger, Rev. Mod. Phys. **80**, 885 (2008).
[4] V. A. Yurovsky, M. Olshanii, and D. S. Weiss, Adv. At., Mol., Opt. Phys. **55**, 61 (2008).
[5] M. Olshanii, Phys. Rev. Lett. **81**, 938 (1998).
[6] T. Bergeman, M. G. Moore, and M. Olshanii, Phys. Rev. Lett. **91**, 163201 (2003).
[7] V. S. Melezhik, J. I. Kim, and P. Schmelcher, Phys. Rev. A **76**, 053611 (2007).
[8] S. Saeidian, V. S. Melezhik, and P. Schmelcher, Phys. Rev. A **77**, 042721 (2008).
[9] M. Girardeau, J. Math. Phys. **1**, 516 (1960).
[10] C. Mora, R. Egger, A. O. Gogolin, and A. Komnik, Phys. Rev. Lett. **93**, 170403 (2004).
[11] C. Mora, R. Egger, and A. O. Gogolin, Phys. Rev. A **71**, 052705 (2005).
[12] C. Mora, A. Komnik, R. Egger, and A. O. Gogolin, Phys. Rev. Lett. **95**, 080403 (2005).
[13] B. E. Granger and D. Blume, Phys. Rev. Lett. **92**, 133202 (2004).
[14] J. I. Kim, V. S. Melezhik, and P. Schmelcher, Phys. Rev. lett. **97**, 193203 (2006).
[15] J. I. Kim, V. S. Melezhik, and P. Schmelcher, Prog. Theor. Phys. Supl. **166**, 159 (2007).
[16] V. S. Melezhik and P. Schmelcher, New J. Phys. **11**, 073031 (2009).
[17] V. S. Melezhik and P. Schmelcher, Phys. Rev. A **84**, 042712 (2011).
[18] M. G. Moore, T. Bergeman, and M. Olshanii, J. Phys. IV **116**, 69 (2004).
[19] P. Giannakeas, V. S. Melezhik, and P. Schmelcher, Phys. Rev. A **84**, 023618 (2011); **85**, 042703 (2012).
[20] P. Giannakeas, F. K. Diakonos, and P. Schmelcher, Phys. Rev. A **86**, 042703 (2012).
[21] T. Kinoshita, T. Wenger, and D. S. Weiss, Science **305**, 1125 (2004).
[22] B. Paredes, A. Widera, V. Murg, O. Mandel, S. Fölling, I. Cirac, G. V. Shlyapnikov, T. W. Hänsch, and I. Bloch, Nature (London) **429**, 277 (2004).
[23] E. Haller, M. Gustavsson, M. J. Mark, J. G. Danzl, R. Hart, G. Pupillo, and H. C. Nägerl, Science **325**, 1224 (2009).
[24] E. Haller, M. J. Mark, R. Hart, J. G. Danzl, L. Reichsöllner, V. Melezhik, P. Schmelcher, and H. C. Nägerl, Phys. Rev. Lett. **104**, 153203 (2010).
[25] H. Moritz, T. Stöferle, K. Guenter, M. Köhl, and T. Esslinger, Phys. Rev. Lett. **94**, 210401 (2005).
[26] K. Günter, T. Stöferle, H. Moritz, M. Köhl, and T. Esslinger, Phys. Rev. Lett. **95**, 230401 (2005).
[27] B. Fröhlich, M. Feld, E. Vogt, M. Koschorreck, W. Zwerger, and M. Köhl, Phys. Rev. Lett. **106**, 105301 (2011).
[28] G. Lamporesi, J. Catani, G. Barontini, Y. Nishida, M. Inguscio, and F. Minardi, Phys. Rev. Lett. **104**, 153202 (2010).
[29] E. Haller, M. Rabie, M. J. Mark, J. G. Danzl, R. Hart, K. Lauber, G. Pupillo, and H. C. Nägerl, Phys. Rev. Lett. **107**, 230404 (2011).
[30] S. G. Peng, S. S. Bohloul, X. J. Liu, H. Hu, and P. D. Drummond, Phys. Rev. A **82**, 063633 (2010); S. G. Peng, H. Hu, X. J. Liu, and P. D. Drummond, *ibid.* **84**, 043619 (2011).
[31] W. Zhang and P. Zhang, Phys. Rev. A **83**, 053615 (2011).
[32] S. Sala, P.-I. Schneider, and A. Saenz, Phys. Rev. Lett. **109**, 073201 (2012).
[33] E. Tiesinga, C. J. Williams, F. H. Mies, and P. S. Julienne, Phys. Rev. A **61**, 063416 (2000); V. A. Yurovsky, *ibid.* **71**, 012709 (2005).
[34] S. Grishkevich, S. Sala, and A. Saenz, Phys. Rev. A **84**, 062710 (2011).
[35] C. Chin, V. Vuletić, A. J. Kerman, S. Chu, E. Tiesinga, P. J. Leo, and C. J. Williams, Phys. Rev. A **70**, 032701 (2004).
[36] A. D. Lange, K. Pilch, A. Prantner, F. Ferlaino, B. Engeser, H.-C. Nägerl, R. Grimm, and C. Chin, Phys. Rev. A **79**, 013622 (2009).
[37] F. H. Mies and M. Raoult, Phys. Rev. A **62**, 012708 (2000).
[38] D. B. M. Dickerscheid and H. T. C. Stoof, Phys. Rev. A **72**, 053625 (2005).
[39] R. B. Diener and T.-L. Ho, Phys. Rev. Lett. **96**, 010402 (2006).
[40] V. A. Yurovsky, Phys. Rev. A **73**, 052709 (2006).
[41] P.-I. Schneider, Y. V. Vanne, and A. Saenz, Phys. Rev. A **83**, 030701(R) (2011).
[42] S.-G. Peng, H. Hu, X.-J. Liu, and K. Jiang, Phys. Rev. A **86**, 033601 (2012).
[43] G. F. Gribakin and V. V. Flambaum, Phys. Rev. A **48**, 546 (1993).
[44] C. A. Regal, C. Ticknor, J. L. Bohn, and D. S. Jin, Nature (London) **424**, 47 (2003).
[45] M. Bartenstein *et al.*, Phys. Rev. Lett. **94**, 103201 (2005).
[46] N. R. Claussen, S. J. J. M. F. Kokkelmans, S. T. Thompson, E. A. Donley, E. Hodby, and C. E. Wieman, Phys. Rev. A **67**, 060701(R) (2003).
[47] S. T. Thompson, E. Hodby, and C. E. Wieman, Phys. Rev. Lett. **95**, 190404 (2005).
[48] S. B. Papp and C. E. Wieman, Phys. Rev. Lett. **97**, 180404 (2006).
[49] V. S. Melezhik and C.-Y. Hu, Phys. Rev. Lett. **90**, 083202 (2003).
[50] J. I. Kim, J. Schmiedmayer, and P. Schmelcher, Phys. Rev. A **72**, 042711 (2005).